A Surrogate-Assisted Evolutionary Algorithm with Geometry-Guided Initialization and Memory-Guided Variation for Expensive Multi-Objective Problems

1st Zitong Su, 2nd Min-Rong Chen
School of Computer Science, South China Normal University, Guangzhou 510631, China
2024023443@m.scnu.edu.cn, mrongchen@126.com

***Abstract*—In recent years, numerous surrogate-assisted evolutionary algorithms (SAEAs) have been developed for expensive multi-objective optimization problems (EMOPs). However, under a stringent evaluation budget, many existing SAEAs are hindered by low-quality initialization, inefficient use of training data for surrogate modeling, and limited exploitation of historical high-quality solutions. This paper proposes an SAEA with geometry-guided initialization and memory-guided variation (GIMV-SAEA). Specifically, a geometry-guided initialization scheme combines boundary probing with a center anchor and early local elite sampling to generate high-quality initial solutions while maintaining uniform exploration. An evolutionary-stage-aware adaptive training set construction strategy is further designed to balance surrogate training cost and predictive accuracy. In addition, a memory-guided variation operator preserves historical elite solutions and applies stronger perturbations to poorly converged decision variables. Experimental results on the DTLZ, WFG, and MaF test suites, as well as offset DTLZ instances, demonstrate that GIMV-SAEA achieves competitive performance on expensive multi- and many-objective optimization.**

***Index Terms*—Expensive multi-objective optimization, geometry-guided initialization, memory-guided variation, surrogate-assisted evolutionary algorithms.**

I. Introduction

Multi- and many-objective optimization problems are prevalent in real-world engineering applications that involve simultaneously optimizing multiple conflicting objectives, such as the trauma system design [1] and neural architecture search of deep neural networks [2]. In these practical applications, objective functions are often evaluated via time-consuming numerical simulations or physical experiments, making the number of affordable function evaluations strictly limited and thus categorizing these problems as expensive multi-objective optimization problems (EMOPs). In recent years, surrogate-assisted evolutionary algorithms (SAEAs) have attracted increasing attention for solving EMOPs.

Despite recent progress, the performance of SAEAs can deteriorate severely when the evaluation budget is extremely limited. In such data-sparse regimes, commonly used initialization methods, such as Latin hypercube sampling (LHS) [3], provide space-filling coverage but ignore problem-relevant geometric priors, often leading to poor early populations and unreliable surrogates that may misguide the search and waste a substantial portion of the scarce evaluation budget. Meanwhile, many surrogate management strategies rely on pre-defined or stage-insensitive training-set construction schemes and struggle to balance the training cost of Kriging models [4] against modeling accuracy as the search progresses. In addition, conventional variation operators rarely exploit historical search information, thereby slowing convergence when only a small number of generations are available.

To address these issues, we propose an SAEA with geometry-guided initialization and memory-guided variation (GIMV-SAEA), which unifies geometry-guided initialization, stage-aware training-set construction, and memory-guided adaptive variation for EMOPs. The main contributions of this paper are summarized as follows:

1) A geometry-guided three-stage initialization (TSI) strategy is proposed as an alternative to standard LHS. By combining boundary probing, a central anchor, global space-filling sampling, and elite-guided exploration, it improves initial decision-space coverage and reduces early surrogate uncertainty.
2) An evolution-stage-aware adaptive training mechanism is developed to dynamically construct training sets from multiple archives, balancing Kriging accuracy and computational cost.
3) A memory-guided adaptive variation operator is designed to learn variable sensitivity from elite archives and bias the search toward promising subspaces, improving convergence under limited budgets.

II. Related Work

A. Surrogate-Assisted Evolutionary Algorithms

SAEAs are designed to solve computationally expensive optimization problems by approximating objective functions with efficient surrogate models [5]. Depending on the role of the surrogate, SAEAs can be broadly categorized into classification-based and regression-based approaches. Classification-based methods, such as CSEA [6], typically

This work was partially supported by the National Natural Science Foundation of China (Grant Nos. 62573201, U23A20303, 62573326, 62533016, 61825203, 62332007, and U22B2028), the Zhejiang Provincial Natural Science Foundation of China (Grant No. LZ25F030007), the Outstanding Youth Project of the Guangdong Basic and Applied Basic Research Foundation (Grant No. 2023B1515020064), and the Guangdong Basic and Applied Basic Research Foundation (Grant No. 2024A1515140109). (Corresponding author: Min-Rong Chen)

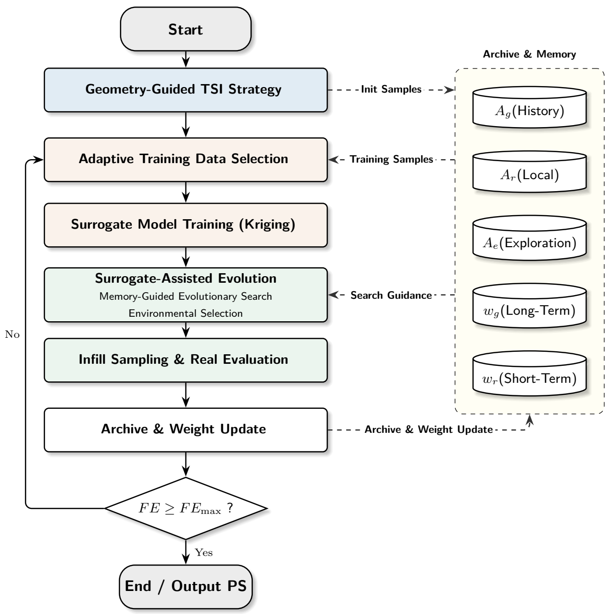

Fig. 1. The general framework of GIMV-SAEA.

use classifiers to predict feasibility or dominance relationships of candidate solutions, filtering out unpromising individuals to save computational resources. Regression-based methods, such as K-RVEA [7] and PIEA [8], instead employ surrogate models including polynomial regression, radial basis function networks, and Kriging models to predict objective values.

B. Kriging Models

The Kriging model treats the objective function as a realization of a stochastic process. Given a set of training data, it provides the linear unbiased prediction (mean) and estimated mean squared error (variance) for any unobserved solution. These properties enable calculation of the Expected Improvement (EI) criterion, which is used in this work to guide infill sampling. Detailed formulations of the Kriging model and EI can be found in the literature [4], [9].

III. Proposed Method

To address cold-start and efficiency challenges in EMOPs, we propose GIMV-SAEA. As illustrated in Fig.1, the framework comprises six modules: Geometry-Guided TSI, Adaptive Training Data Selection, Kriging model training, Surrogate-Assisted Evolution, Infill Sampling, and Archive & Weight Update. The overall budget-driven workflow is summarized in Algorithm 1, which iteratively executes these components until the evaluation budget is exhausted.

Algorithm 1 General Framework of GIMV-SAEA

Input: evaluation budget $FE_{\max}$; population size N; inner generations $w_{\max}$; initial sample size N_{init}; training set size N_{train}; infill batch size μ; geometry-init parameters (ρ, κ); memory factor α_{mem}; diversity threshold τ
Output: Global archive A (evaluated solutions)

$A \leftarrow \text{GeometryGuidedTSI}(N_{\text{init}}, \rho, \kappa)$
$FE \leftarrow |A|$
$(A_g, A_r, A_e) \leftarrow \text{UpdateArchive}(A)$
$(\mathbf{w}_g, \mathbf{w}_r) \leftarrow \text{UpdateWeights}(A_g, \alpha_{\text{mem}})$
while $FE < FE_{\max}$ **do**
  $\mathcal{C} \leftarrow (A, A_g, A_r, A_e, FE, FE_{\max}, N_{\text{init}})$
  $D_{\text{train}} \leftarrow \text{AdaptiveTrainingDataSelection}(\mathcal{C}, N_{\text{train}})$
  Train Kriging models $\mathcal{M}$ using D_{train}
  $P \leftarrow$ decision vectors in D_{train}
  for $gen = 1$ **to** $w_{\max}$ **do**
    $O \leftarrow \text{MemoryGuidedOperator}(P, \mathbf{w}_g, \mathbf{w}_r, \tau)$
    $\hat{\mathbf{f}} \leftarrow$ Evaluate $P \cup O$ using surrogate models $\mathcal{M}$
    $P \leftarrow \text{EnvironmentalSelection}(P \cup O, \hat{\mathbf{f}}, N)$
  end for
  $X \leftarrow \text{InfillSampling}(P, \mu)$
  $S \leftarrow$ Evaluate X using real objective functions $\mathbf{F}$
  $FE \leftarrow FE + |X|, \quad A \leftarrow A \cup S$
  $(A_g, A_r, A_e) \leftarrow \text{UpdateArchive}(A)$
  $(\mathbf{w}_g, \mathbf{w}_r) \leftarrow \text{UpdateWeights}(A_g, \alpha_{\text{mem}})$
end while

A. Geometry-Guided Three-Stage Initialization

To alleviate the cold-start problem caused by geometry-agnostic initialization in EMOPs, we propose a geometry-guided three-stage initialization. The design of TSI is motivated by the empirical regularity of the Pareto set (PS), which often forms low-dimensional manifolds in the decision space and may intersect decision-space boundaries or traverse interior regions [10]. Motivated by this, we treat decision-space boundaries and the central anchor as lightweight geometric priors to mitigate cold-start uncertainty under strict budgets. As illustrated in Fig. 2, TSI constructs the initial population through three stages.

1) Stage 1 Systematic Probing (Axis-Parallel Boundary Probing): With $2D+1$ evaluations, TSI first probes axis-parallel boundaries. The center point is defined as

$$\mathbf{x}_j^c = \frac{L_j + U_j}{2}, \quad j = 1, \dots, D, \tag{1}$$

where L_j and U_j denote the lower and upper bounds of the j-th decision variable, respectively. For each dimension i, two boundary probes are generated by setting the i-th component of $\mathbf{x}^c$ to L_i and U_i, denoted by $\mathbf{x}^{L,i}$ and $\mathbf{x}^{U,i}$, respectively. The probing set is

$$\mathcal{P}_1 = \{\mathbf{x}^c\} \cup \bigcup_{i=1}^{D} \{\mathbf{x}^{L,i}, \mathbf{x}^{U,i}\}. \tag{2}$$

2) Stage 2 LHS Exploration (Global Uniform Sampling): To ensure global coverage, TSI adds space-filling samples via LHS. Given a total initialization budget N_{init}, the number of LHS samples is

$$N_{\text{LHS}} = \left\lceil \rho \cdot \left(N_{\text{init}} - (2D+1)\right) \right\rceil, \tag{3}$$

where ρ is set to 0.5 in this study. This yields $\mathcal{P}_2$ and the intermediate population $\mathcal{P}_{\text{temp}} = \mathcal{P}_1 \cup \mathcal{P}_2$.

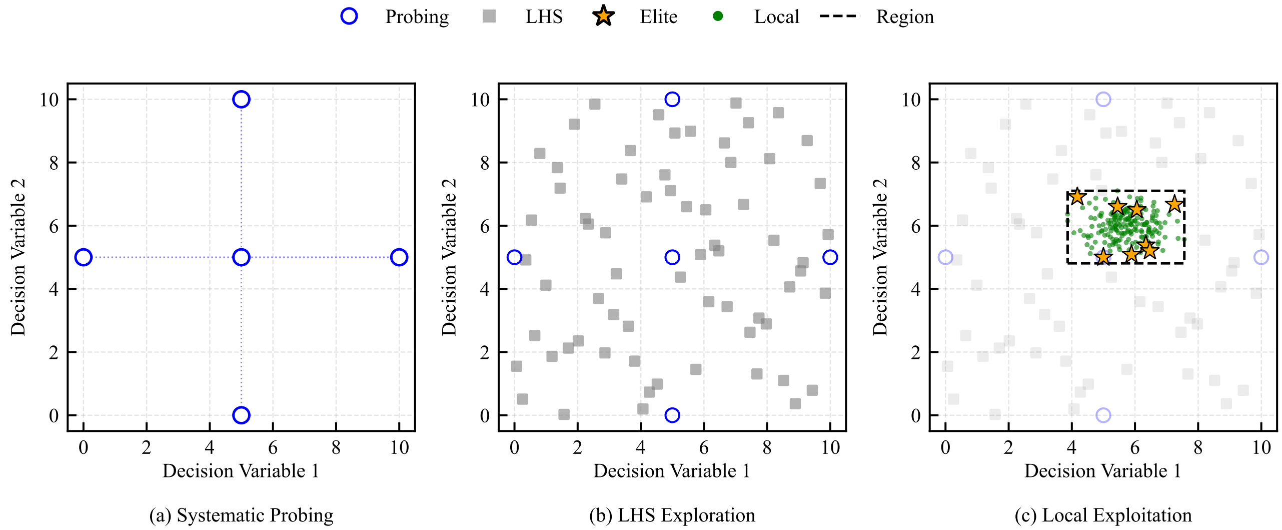

Fig. 2. Schematic illustration of the proposed Geometry-Guided Three-Stage Initialization ($D = 2$). It consists of three stages: (a) systematic probing, (b) global LHS exploration, and (c) elite-guided Gaussian densification, which jointly ensure boundary coverage and internal diversity.

Note that TSI retains a space-filling component (Stage 2) to avoid over-committing to geometric priors; robustness under offset settings is reported in Section IV-F.

3) Stage 3 Local Exploitation (Elite-Guided Gaussian Densification): The remaining budget is computed as

$$N_{\text{local}} = \max\big(0,\ N_{\text{init}} - |\mathcal{P}_{\text{temp}}|\big). \tag{4}$$

If $N_{\text{local}} > 0$, we select $N_{\text{elite}} = \lceil \kappa\, |\mathcal{P}_{\text{temp}}| \rceil$ elite solutions ($\kappa = 0.2$) using APD [11] for $M \leq 6$, or NDSort-CD [12] otherwise.

Let X_{elite} denote the elite decision vectors. An expanded elite envelope is constructed by enlarging the axis-aligned bounding box of X_{elite} around its center (with expansion factor 1.1 and clipped to the original bounds). Within this envelope, a diagonal Gaussian with mean $\boldsymbol{\mu}$ and standard deviation $\boldsymbol{\sigma}$ (each lower bounded by 10^{-3}) is estimated from the elite solutions and used to generate N_{local} samples, which are then projected back to the envelope. Let $\mathcal{P}_{\text{local}}$ denote these samples. Finally,

$$\mathcal{P}_{\text{init}} = \mathcal{P}_{\text{temp}} \cup \mathcal{P}_{\text{local}}. \tag{5}$$

B. Evolutionary Stage-Aware Training Set Construction

Training a Kriging model surrogate scales cubically with the training size. To balance model fidelity and efficiency within a limited budget, we construct a compact training set based on evolutionary progress.

1) Three-archive mechanism: Based on the global history archive A, we maintain three complementary archives: A_g for global elites, A_r for recent solutions, and A_e for exploration. All three archives are initially populated with solutions evaluated during the three-stage initialization. Subsequently, they are updated online: A_g via non-dominated sorting with RVEA-style APD selection to preserve globally competitive solutions; A_r in a FIFO manner to track the recent search trajectory, where the μ newly evaluated solutions replace the μ oldest ones once the capacity is reached; and A_e by mining solutions from A with the largest Euclidean nearest-neighbor distances to $A_g \cup A_r$, thereby improving spatial coverage. The sizes of these archives are fixed throughout the run and are specified in Section IV-A.

2) Evolutionary progress: We define the progress indicator p based on the current number of function evaluations (FE):

$$p = \frac{FE - N_{\text{init}}}{FE_{\max} - N_{\text{init}}}, \tag{6}$$

where N_{init} is the initialization size. Based on p, the training set is constructed in three phases.

a) Phase 1 Exploration ($p < 0.3$): To maximize global coverage with scarce data, we use the full history: $D_{\text{train}} = A$.

b) Phase 2 Transition ($0.3 \leq p < 0.7$): We employ a hybrid candidate pool combining the three archives with $\text{TopLayers}(A)$, which denotes the union of the first five non-dominated fronts in A: $D_{\text{train}} = \text{TopLayers}(A) \cup A_g \cup A_r \cup A_e$.

c) Phase 3 Convergence ($p \geq 0.7$): We restrict the training set to the three archives to emphasize local accuracy near the current PF approximation: $D_{\text{train}} = A_g \cup A_r \cup A_e$. If needed, unselected candidates with the smallest APD values are added until N_{train} is reached.

3) RVEA-style APD Truncation: Across all phases, duplicate decision vectors are removed to improve numerical stability. If $|D_{\text{train}}| > N_{\text{train}}$, we apply RVEA-style APD filtering with reference-vector association to retain N_{train} well-distributed samples in the objective space, reducing the risk of ill-conditioned Kriging model correlation matrices.

C. Memory-Guided Adaptive Variation Operator

To enhance decision-space guidance in EMOPs, we propose a memory-guided adaptive variation operator that learns variable-wise importance from elite solutions and biases polynomial mutation. We use simulated binary crossover (SBX) for recombination and polynomial mutation for perturbation. In addition, elite solutions randomly sampled from A_g may be injected into the offspring population with a probability p_{inj} to promote exploitation of high-quality regions.

1) Dual Weight Memories: Two complementary weight vectors, $\{\mathbf{w}_g, \mathbf{w}_r\} \in \mathbb{R}^D$, are maintained to capture long-term and short-term variable importance, respectively. For each variable j, its importance is estimated from the normalized dispersion over elites:

$$s_j = \exp\left(-\gamma \frac{\text{std}(\mathbf{x}_j)}{U_j - L_j}\right), \quad \mathbf{x}_j = \{x_j^{(i)} \mid i \in A_g\}, \tag{7}$$

where L_j and U_j are variable bounds and $\gamma = 20$.

The importance scores are ranked in descending order. Let π be a permutation such that $s_{\pi_1} \geq \cdots \geq s_{\pi_D}$. To avoid unstable guidance with limited elites, we set $K = 8$ for $D = 20$, with $K_g = 3$ and $K_r = 5$ for the global and recent memories, respectively. For other decision-space dimensions, we set $K = \min(D, \max(2, \text{round}(0.4D)))$ and assign K_g and K_r in a 3:5 ratio. With $\mathbf{w}_0 = \mathbf{1}$ and $\xi_j \sim \mathcal{U}(-\varepsilon, \varepsilon)$ ($\varepsilon = 0.05$), the target weights are

$$\tilde{w}_{g,j} = \begin{cases} w_{0,j} + s_j, & j \in \mathcal{I}_g, \\ w_{0,j}, & \text{otherwise}, \end{cases} \tag{8}$$

$$\tilde{w}_{r,j} = \begin{cases} w_{0,j} + s_j + \xi_j, & j \in \mathcal{I}_r, \\ w_{0,j}, & \text{otherwise}. \end{cases} \tag{9}$$

The memories are updated via exponential smoothing:

$$\begin{aligned} \mathbf{w}_g &\leftarrow \alpha_{\text{mem}} \mathbf{w}_g + (1 - \alpha_{\text{mem}}) \tilde{\mathbf{w}}_g, \\ \mathbf{w}_r &\leftarrow (1 - \alpha_{\text{mem}}) \mathbf{w}_r + \alpha_{\text{mem}} \tilde{\mathbf{w}}_r, \end{aligned} \tag{10}$$

where $\alpha_{\text{mem}} = 0.7$. The asymmetric smoothing scheme is intentionally designed to model two time scales: the global memory $\mathbf{w}_g$ evolves slowly to capture long-term variable importance, while the recent memory $\mathbf{w}_r$ reacts more quickly to new elite patterns, enabling rapid adaptation to changes in search dynamics.

2) Adaptive Mode Switching: To adapt the mutation behavior to the search state, we measure the normalized population diversity as follows:

$$\Delta = \frac{1}{D} \sum_{j=1}^{D} \frac{\text{std}(\mathbf{p}_j)}{U_j - L_j}, \tag{11}$$

where $\mathbf{p}_j$ collects the j-th decision-variable values of the parent population. If $\Delta < \tau$, the operator switches to *Polarization Mode*; otherwise, it remains in *Robust Mode*. In our implementation, $\tau = 0.02$.

3) Memory-Guided Variation: According to the current search mode, the two memories are aggregated as $\mathbf{w} = \text{norm}((\mathbf{w}_g + \mathbf{w}_r)/2)$, where $\text{norm}(\cdot)$ scales a vector to $[0, 1]$. In *Robust Mode*, the mutation distribution index is set to $\eta_{m,j} = 20 + 5w_j$ for all offspring, and elite injection is applied with probability $p_{\text{inj}} = 0.01$. In *Polarization Mode*, offspring are divided into three groups with proportions 0.3/0.3/0.4: *Exploration* ($\eta_{m,j} = 2$), *Buffer* ($\eta_{m,j} = 20 + 10w_j$), and *Refinement* ($\eta_{m,j} = 50 + 20w_j$), with elite injection probability $p_{\text{inj}} = 0.3$. As a result, variables with larger weights are mutated more conservatively, whereas those with smaller weights receive stronger perturbations to encourage exploration.

D. Environmental Selection and Infill Sampling

Following standard practice, we adopt environmental selection and batch infill sampling modules similar to those used in K-RVEA and ParEGO [9].

1) Environmental Selection: We adopt the environmental selection strategy of K-RVEA. Specifically, solutions are associated with reference vectors by the smallest-angle rule, and for each reference vector, the solution with the minimum APD is kept for the next generation.

2) Infill Sampling: We employ a ParEGO-inspired infill criterion [9] to select μ solutions for expensive evaluation. The candidate pool is derived from the final internal population P after $w_{\max}$ surrogate-assisted generations (Algorithm 1). Candidates whose decision-space distance to previously evaluated solutions is below 10^{-6} are discarded. At each selection round, a random weight vector is generated, and the predicted objective means are scalarized by the Tchebycheff function with respect to the ideal point of the current candidate pool. The variance of the scalarized prediction is approximated by the weighted sum of the objective-wise prediction variances, and EI is evaluated by the standard Gaussian criterion for minimization. The candidate with the largest EI is selected and removed from the pool.

IV. Experimental Studies

This section evaluates GIMV-SAEA against six state-of-the-art SAEAs, including PIEA [8], SFADE [13], ESBCEO [14], PCSAEA [15], REMO [16], and K-RVEA [7].

A. Experimental Settings

Experiments are conducted on 90 test instances from the DTLZ [17], WFG [18], and MaF [19] test suites with $M \in \{3, 4, 6, 8, 10\}$. For $M = 3$, the number of decision variables is set to $D = 20$ for all problems. For $M > 3$, we use $D = 20$ for all problems except WFG2 and WFG3, where $D = 21$. For each instance, the maximum number of expensive function evaluations is set to $FE_{\max} = 300$. The population size, initialization budget, training set size, and number of inner generations are set to $N = N_{\text{init}} = N_{\text{train}} = 100$ and $w_{\max} = 20$. For GIMV-SAEA, the capacities of the global, recent, and exploration archives are set to $|A_g| = 40$, $|A_r| = 20$, and $|A_e| = 100$, respectively, and the number of infill samples per iteration is $\mu = 5$. All algorithms use the same initialization budget N_{init}. GIMV-SAEA allocates the budget across the three stages of TSI, whereas the baseline algorithms allocate the entire budget to LHS. All compared algorithms follow the parameter settings recommended in their original publications and corresponding PlatEMO [20] implementations, without any problem-specific tuning.

TABLE I
IGD$^+$ RESULTS (MEAN AND STANDARD DEVIATION) OBTAINED BY GIMV-SAEA AND SIX COMPARED ALGORITHMS ON DTLZ AND MAF BENCHMARK PROBLEMS. THE BEST MEAN IN EACH ROW IS HIGHLIGHTED; "+", "−", AND "≈" DENOTE BETTER, WORSE, AND SIMILAR PERFORMANCE VERSUS GIMV-SAEA.

Problem	M	KRVEA	REMO	PCSAEA	ESBCEO	SFADE	PIEA	GIMV-SAEA
DTLZ1	3	3.0417e+2 (4.97e+1) -	2.0424e+2 (4.42e+1) -	3.2039e+2 (5.14e+1) -	2.0249e+2 (2.52e+1) -	1.9515e+2 (2.53e+1) -	1.7006e+2 (3.10e+1) -	**9.5442e-2 (3.03e-5)**
	4	2.8178e+2 (4.00e+1) -	1.9322e+2 (3.43e+1) -	2.9263e+2 (3.17e+1) -	1.7073e+2 (3.16e+1) -	1.8836e+2 (2.12e+1) -	1.3684e+2 (2.02e+1) -	**1.1468e-1 (5.70e-5)**
	6	2.1844e+2 (2.93e+1) -	1.3763e+2 (2.48e+1) -	2.3321e+2 (3.30e+1) -	1.3410e+2 (3.85e+1) -	1.3857e+2 (2.34e+1) -	1.1522e+2 (1.89e+1) -	**1.5456e-1 (2.85e-4)**
	8	1.6940e+2 (2.02e+1) -	9.0355e+1 (2.12e+1) -	1.9143e+2 (2.44e+1) -	1.0533e+2 (3.45e+1) -	1.2305e+2 (2.06e+1) -	1.1579e+2 (3.26e+1) -	**1.8344e-1 (9.58e-4)**
	10	1.0437e+2 (2.27e+1) -	5.9504e+1 (1.12e+1) -	1.4258e+2 (2.80e+1) -	9.7785e+1 (2.68e+1) -	9.7578e+1 (1.85e+1) -	8.5510e+1 (1.94e+1) -	**2.0256e-1 (1.52e-3)**
DTLZ2	3	8.5545e-1 (1.18e-1) -	3.3879e-1 (8.14e-2) -	6.9540e-1 (8.38e-2) -	5.3084e-1 (6.54e-2) -	1.3415e-1 (2.03e-2) -	2.4534e-1 (3.07e-2) -	**5.3578e-2 (6.43e-3)**
	4	9.1007e-1 (6.03e-2) -	4.7801e-1 (9.63e-2) -	8.0910e-1 (6.08e-2) -	5.9215e-1 (5.11e-2) -	2.8790e-1 (2.94e-2) -	2.9587e-1 (2.95e-2) -	**8.8286e-2 (8.35e-3)**
	6	8.4031e-1 (6.40e-2) -	5.2365e-1 (8.36e-2) -	8.5995e-1 (5.53e-2) -	7.3115e-1 (5.69e-2) -	4.4757e-1 (2.45e-2) -	4.0524e-1 (2.73e-2) -	**1.7207e-1 (1.72e-2)**
	8	7.3963e-1 (7.62e-2) -	5.7580e-1 (6.11e-2) -	8.8665e-1 (5.23e-2) -	7.8135e-1 (3.11e-2) -	5.5026e-1 (3.07e-2) -	5.0129e-1 (2.57e-2) -	**2.4610e-1 (2.26e-2)**
	10	6.8328e-1 (7.54e-2) -	5.7657e-1 (5.97e-2) -	8.5541e-1 (2.87e-2) -	7.6009e-1 (3.13e-2) -	6.6684e-1 (3.18e-2) -	5.2320e-1 (1.92e-2) -	**2.9682e-1 (3.09e-2)**
DTLZ3	3	9.1056e+2 (1.16e+2) -	6.5268e+2 (1.36e+2) -	9.4549e+2 (7.86e+1) -	4.2356e+2 (6.06e+1) -	4.4305e+2 (1.61e+1) -	4.3063e+2 (1.86e+1) -	**2.2315e-1 (1.12e-3)**
	4	8.4818e+2 (8.81e+1) -	6.5014e+2 (1.06e+2) -	9.2754e+2 (1.26e+2) -	3.9070e+2 (6.41e+1) -	4.0479e+2 (4.24e+1) -	4.1464e+2 (2.95e+1) -	**3.2714e-1 (8.21e-4)**
	6	6.7073e+2 (9.42e+1) -	4.4332e+2 (1.22e+2) -	7.9551e+2 (9.26e+1) -	3.5381e+2 (6.71e+1) -	3.4623e+2 (2.31e+1) -	3.6196e+2 (1.37e+1) -	**4.6545e-1 (8.74e-5)**
	8	5.2643e+2 (6.49e+1) -	3.4572e+2 (7.35e+1) -	6.5357e+2 (6.49e+1) -	2.4647e+2 (1.10e+2) -	2.8465e+2 (6.29e+1) -	3.0822e+2 (1.35e+1) -	**5.6852e-1 (1.78e-5)**
	10	3.8418e+2 (6.32e+1) -	2.4708e+2 (6.74e+1) -	4.8874e+2 (6.63e+1) -	2.4926e+2 (5.23e+1) -	2.4226e+2 (2.27e+1) -	2.5345e+2 (2.57e+1) -	**6.1103e-1 (2.66e-4)**
DTLZ4	3	1.0222e+0 (8.92e-2) -	4.9229e-1 (1.20e-1) -	7.9305e-1 (8.51e-2) -	9.2369e-1 (1.31e-1) -	5.1758e-1 (6.00e-3) -	5.1911e-1 (3.91e-2) -	**6.9979e-2 (7.58e-3)**
	4	9.7599e-1 (8.59e-2) -	4.4471e-1 (6.56e-2) -	9.0207e-1 (1.02e-1) -	9.1220e-1 (1.35e-1) -	5.9097e-1 (3.34e-2) -	6.1464e-1 (1.01e-2) -	**9.9890e-2 (7.72e-3)**
	6	9.8712e-1 (1.05e-1) -	4.8808e-1 (7.17e-2) -	9.8610e-1 (6.64e-2) -	8.7114e-1 (9.54e-2) -	6.8939e-1 (4.68e-2) -	7.0250e-1 (3.57e-2) -	**1.5115e-1 (7.77e-3)**
	8	8.4079e-1 (8.44e-2) -	5.2329e-1 (6.72e-2) -	9.6589e-1 (7.42e-2) -	8.7395e-1 (6.80e-2) -	7.4304e-1 (5.44e-2) -	7.4429e-1 (5.82e-2) -	**1.8899e-1 (6.31e-3)**
	10	7.8367e-1 (8.05e-2) -	5.1228e-1 (6.52e-2) -	8.7505e-1 (5.91e-2) -	8.0417e-1 (6.68e-2) -	7.6598e-1 (5.75e-2) -	7.2958e-1 (7.13e-2) -	**2.3525e-1 (5.79e-3)**
DTLZ5	3	7.5153e-1 (1.26e-1) -	3.2560e-1 (8.05e-2) -	6.0027e-1 (8.24e-2) -	4.8143e-1 (7.52e-2) -	7.0467e-2 (1.47e-2) -	1.5876e-1 (2.57e-2) -	**2.5345e-2 (4.42e-3)**
	4	7.4481e-1 (7.11e-2) -	3.8898e-1 (1.06e-1) -	6.5545e-1 (6.67e-2) -	4.4767e-1 (6.79e-2) -	7.2336e-2 (1.66e-2) -	1.3842e-1 (3.99e-2) -	**2.0244e-2 (5.65e-3)**
	6	5.7473e-1 (7.00e-2) -	3.4539e-1 (8.33e-2) -	5.9267e-1 (6.06e-2) -	4.1613e-1 (5.64e-2) -	4.6712e-2 (1.09e-2) -	1.2280e-1 (1.75e-2) -	**1.5669e-2 (5.04e-3)**
	8	3.8741e-1 (7.14e-2) -	2.6547e-1 (6.69e-2) -	4.7989e-1 (6.09e-2) -	3.4217e-1 (4.47e-2) -	5.3921e-2 (1.28e-2) -	9.5979e-2 (1.33e-2) -	**1.4104e-2 (4.03e-3)**
	10	2.9253e-1 (6.33e-2) -	1.9421e-1 (5.08e-2) -	3.9592e-1 (4.12e-2) -	2.9288e-1 (4.47e-2) -	7.5369e-2 (2.13e-2) -	8.0040e-2 (1.81e-2) -	**1.4573e-2 (6.17e-3)**
DTLZ6	3	1.0869e+1 (6.18e-1) -	1.2309e+1 (8.97e-1) -	1.4586e+1 (4.10e-1) -	6.4093e+0 (1.26e+0) +	6.5717e+0 (1.51e+0) +	**3.7333e+0 (1.44e+0) +**	9.1074e+0 (1.09e+0)
	4	9.8814e+0 (8.17e-1) -	1.2350e+1 (8.46e-1) -	1.3796e+1 (3.36e-1) -	6.8474e+0 (1.18e+0) +	5.9033e+0 (1.55e+0) +	**3.1115e+0 (1.42e+0) +**	8.6268e+0 (6.99e-1)
	6	9.4199e+0 (6.29e-1) -	1.0649e+1 (9.62e-1) -	1.2266e+1 (5.46e-1) -	5.7408e+0 (1.43e+0) +	4.3054e+0 (1.59e+0) +	**2.8478e+0 (1.58e+0) +**	7.9886e+0 (9.04e-1)
	8	8.3079e+0 (7.17e-1) -	9.2218e+0 (6.88e-1) -	1.0434e+1 (3.46e-1) -	4.6858e+0 (1.18e+0) +	3.3769e+0 (1.43e+0) +	**2.3727e+0 (1.23e+0) +**	6.8808e+0 (6.02e-1)
	10	6.8812e+0 (6.08e-1) ≈	7.7237e+0 (6.79e-1) -	8.6945e+0 (3.91e-1) -	4.1158e+0 (7.96e-1) +	3.1401e+0 (9.90e-1) +	**1.6964e+0 (9.19e-1) +**	6.5442e+0 (6.48e-1)
DTLZ7	3	**1.1033e-1 (1.46e-2) ≈**	2.3869e+0 (6.00e-1) -	6.7100e+0 (1.01e+0) -	3.8426e+0 (1.53e+0) -	3.9037e-1 (2.65e-1) -	2.8440e+0 (8.03e-1) -	1.5950e-1 (7.00e-2)
	4	**2.8879e-1 (3.22e-2) +**	4.5864e+0 (9.94e-1) -	9.6735e+0 (8.03e-1) -	4.0092e+0 (2.39e+0) -	6.3384e-1 (8.90e-2) -	4.8560e+0 (1.44e+0) -	3.8390e-1 (1.76e-1)
	6	**6.3963e-1 (4.89e-2) ≈**	8.5637e+0 (1.41e+0) -	1.5935e+1 (1.22e+0) -	3.8829e+0 (3.53e+0) -	9.1143e-1 (9.87e-2) -	9.4018e+0 (1.71e+0) -	7.0940e-1 (2.96e-1)
	8	8.4732e-1 (8.69e-2) -	1.2644e+1 (2.23e+0) -	1.9237e+1 (3.14e+0) -	8.3995e+0 (4.82e+0) -	1.0061e+0 (1.12e-1) -	1.1618e+1 (2.34e+0) -	**7.6513e-1 (1.13e-1)**
	10	**1.1122e+0 (5.60e-2) +**	1.4399e+1 (2.63e+0) -	2.1866e+1 (3.64e+0) -	5.1261e+0 (3.76e+0) -	1.5745e+0 (2.52e-1) -	1.2231e+1 (5.02e+0) -	1.3817e+0 (3.59e-1)
MaF5	3	3.0212e+0 (4.55e-1) -	1.4242e+0 (2.98e-1) -	2.7386e+0 (7.76e-1) -	3.8792e+0 (8.89e-1) -	3.1635e+0 (1.01e+0) -	4.0333e+0 (4.14e-1) -	**2.3372e-1 (4.14e-2)**
	4	3.6310e+0 (1.14e+0) -	1.8773e+0 (4.22e-1) -	3.1785e+0 (4.79e-1) -	4.0914e+0 (1.25e+0) -	4.6398e+0 (2.20e+0) -	7.1607e+0 (2.43e+0) -	**4.4275e-1 (4.40e-2)**
	6	4.2550e+0 (1.81e+0) -	2.2978e+0 (1.09e+0) -	3.6957e+0 (7.67e-1) -	3.8967e+0 (6.43e-1) -	4.7570e+0 (9.34e-1) -	2.0477e+1 (1.39e+1) -	**9.2391e-1 (4.90e-2)**
	8	3.6714e+0 (1.16e+0) -	3.4128e+0 (1.73e+0) -	4.1166e+0 (1.78e+0) -	3.3178e+0 (7.37e-1) -	3.8955e+0 (9.12e-1) -	5.4280e+1 (4.89e+1) -	**1.2419e+0 (2.73e-2)**
	10	5.3863e+0 (3.16e+0) -	5.1217e+0 (3.07e+0) -	5.4673e+0 (2.81e+0) -	3.5763e+0 (6.67e-1) -	3.8465e+0 (1.27e+0) -	6.3793e+1 (1.19e+2) -	**1.4009e+0 (2.08e-2)**
MaF13	3	1.3937e+0 (5.58e-1) -	7.3992e-1 (1.96e-1) -	1.7592e+0 (3.01e-1) -	1.0207e+0 (2.16e-1) -	3.4145e-1 (5.14e-2) -	4.9122e-1 (3.70e-2) -	**2.3452e-1 (1.19e-3)**
	4	1.1300e+3 (1.59e+3) -	2.0443e+0 (1.18e+0) -	1.8325e+1 (2.44e+1) -	1.4461e+3 (4.33e+3) -	1.9195e+0 (4.77e+0) -	6.4807e-1 (9.45e-2) -	**5.1350e-1 (3.44e-3)**
	6	1.5211e+3 (1.72e+3) -	3.7828e+0 (4.24e+0) -	3.1527e+1 (3.10e+1) -	1.9528e+3 (3.71e+3) -	1.2729e+0 (6.59e-1) -	8.3333e-1 (1.34e-1) -	**5.3003e-1 (3.18e-2)**
	8	2.7814e+3 (3.15e+3) -	5.4777e+1 (2.29e+2) -	6.5296e+1 (9.23e+1) -	3.6841e+3 (7.39e+3) -	1.1598e+0 (4.12e-1) -	1.0298e+0 (1.91e-1) -	**5.8667e-1 (2.28e-3)**
	10	2.4576e+3 (2.42e+3) -	6.9447e+0 (8.24e+0) -	8.2794e+1 (1.00e+2) -	3.0453e+3 (6.03e+3) -	1.0342e+0 (5.02e-1) -	1.3180e+0 (4.63e-1) -	**6.1439e-1 (1.57e-3)**
+/ −/ ≈		2/40/3	0/45/0	0/45/0	5/40/0	5/40/0	5/40/0	

Each algorithm is independently run 20 times for fair comparison. Performance on benchmark problems is evaluated by IGD$^+$ [21], while HV [22] is used for the real-world engineering problem; both are computed using the default PlatEMO implementations. Statistical significance is examined by the Wilcoxon rank-sum test [23] at the 0.05 significance level, where "+", "−", and "≈" indicate that the compared algorithm performs significantly better than, worse than, or similarly to GIMV-SAEA. All algorithms are implemented in PlatEMO and executed on an AMD Ryzen 7 9700X CPU with 32 GB RAM using MATLAB R2025b. PlatEMO v4.12 used in our experiments is publicly available.

B. Comparison with State-of-the-Art Algorithms

Tables I–II report the comparative results of GIMV-SAEA and six state-of-the-art algorithms, namely PIEA, SFADE, ESBCEO, PCSAEA, REMO, and K-RVEA. Across the 90 test instances, GIMV-SAEA achieves the best IGD$^+$ performance in 70 cases, followed by PIEA (9) and REMO (5). REMO performs particularly well on WFG1, likely because its relation-based selection can better identify promising candidates when dominance relations are learned reliably, whereas GIMV-SAEA consistently outperforms the other five competitors on most instances in this suite. On DTLZ7, K-RVEA shows mixed but still competitive results, likely due to its reference-vector-guided selection and adaptive angle-based distance criterion, which are well suited to disconnected Pareto fronts. By contrast, GIMV-SAEA is less competitive on DTLZ6 than recent methods such as PIEA and SFADE, possibly because the complex geometry and strong nonlinearity of DTLZ6 pose a challenge to the current geometry-guided initialization. Overall, the combination of Stage 1 boundary probing and central anchoring, Stage 2 space-filling safeguards, and Stage 3 local sampling around early elites helps explain the strong performance of GIMV-SAEA under strictly limited evaluation budgets.

C. Ablation Studies

To assess the contribution of individual components, we compare GIMV-SAEA with three variants, namely *GIMV-LHS* (LHS-based initialization), *GIMV-KRVEA* (K-RVEA-based training), and *GIMV-GA* (standard genetic-algorithm operators), on DTLZ instances with $M = 3$. These instances involve multimodality, bias, and disconnected Pareto fronts,

TABLE II

IGD$^+$ RESULTS (MEAN AND STANDARD DEVIATION) OBTAINED BY GIMV-SAEA AND SIX COMPARED ALGORITHMS ON WFG BENCHMARK PROBLEMS. THE BEST MEAN IN EACH ROW IS HIGHLIGHTED; "+", "−", AND "≈" DENOTE BETTER, WORSE, AND SIMILAR PERFORMANCE VERSUS GIMV-SAEA.

Problem	M	KRVEA	REMO	PCSAEA	ESBCEO	SFADE	PIEA	GIMV-SAEA
WFG1	3	1.7592e+0 (7.63e-2) -	**1.6253e+0 (5.36e-2) +**	2.0905e+0 (7.38e-2) -	2.0453e+0 (7.76e-2) -	1.8126e+0 (8.48e-2) -	1.6324e+0 (3.68e-2) +	1.6935e+0 (6.84e-2)
	4	2.0675e+0 (7.23e-2) -	**1.8634e+0 (7.12e-2) +**	2.2936e+0 (5.84e-2) -	2.2696e+0 (8.43e-2) -	2.0719e+0 (8.11e-2) -	2.2630e+0 (9.16e-2) -	1.9530e+0 (6.52e-2)
	6	2.3826e+0 (7.25e-2) -	**2.2654e+0 (1.01e-1) +**	2.5960e+0 (5.24e-2) -	2.5726e+0 (6.80e-2) -	2.4169e+0 (8.27e-2) -	2.5182e+0 (6.33e-2) -	2.3211e+0 (7.29e-2)
	8	2.6997e+0 (5.87e-2) -	**2.5654e+0 (9.31e-2) +**	2.8704e+0 (3.52e-2) -	2.8654e+0 (5.77e-2) -	2.6668e+0 (5.43e-2) ≈	2.7774e+0 (4.43e-2) -	2.6464e+0 (4.48e-2)
	10	3.0282e+0 (4.08e-2) -	**2.8061e+0 (1.35e-1) +**	3.1135e+0 (4.18e-2) -	3.1472e+0 (3.63e-2) -	3.0245e+0 (5.00e-2) -	3.0476e+0 (3.46e-2) -	2.9773e+0 (3.40e-2)
WFG2	3	6.9283e-1 (3.86e-2) -	6.1913e-1 (5.36e-2) -	7.0462e-1 (5.40e-2) -	7.2599e-1 (5.83e-2) -	8.2855e-1 (8.22e-2) -	1.1022e+0 (1.13e-1) -	**2.9585e-1 (8.76e-3)**
	4	9.3183e-1 (6.62e-2) -	7.6132e-1 (1.51e-1) -	1.0199e+0 (8.94e-2) -	9.7462e-1 (1.00e-1) -	1.0344e+0 (7.62e-2) -	6.8653e-1 (7.50e-2) -	**3.4654e-1 (1.21e-2)**
	6	1.1991e+0 (9.40e-2) -	1.3595e+0 (5.47e-1) -	1.5342e+0 (3.33e-1) -	1.4363e+0 (2.79e-1) -	1.5196e+0 (2.20e-1) -	8.6983e-1 (1.39e-1) -	**4.2203e-1 (2.48e-2)**
	8	1.4744e+0 (1.70e-1) -	2.1531e+0 (7.92e-1) -	2.4058e+0 (5.09e-1) -	1.6553e+0 (3.50e-1) -	1.9211e+0 (2.41e-1) -	1.2737e+0 (3.45e-1) -	**5.8529e-1 (4.49e-2)**
	10	1.6991e+0 (1.73e-1) -	2.8601e+0 (1.13e+0) -	3.4734e+0 (5.72e-1) -	3.1232e+0 (5.27e-1) -	3.3557e+0 (7.56e-1) -	1.5239e+0 (3.71e-1) -	**7.8528e-1 (1.61e-1)**
WFG3	3	7.4476e-1 (2.62e-2) -	6.1496e-1 (3.66e-2) -	6.7220e-1 (2.63e-2) -	6.3278e-1 (2.72e-2) -	6.7601e-1 (4.76e-2) -	**3.2827e-1 (2.68e-2) ≈**	3.4228e-1 (9.15e-3)
	4	8.9741e-1 (2.86e-2) -	7.1319e-1 (6.39e-2) -	8.4292e-1 (3.55e-2) -	7.6913e-1 (4.72e-2) -	8.0667e-1 (5.19e-2) -	5.1495e-1 (4.87e-2) -	**3.9245e-1 (1.34e-2)**
	6	1.1185e+0 (4.77e-2) -	9.2253e-1 (7.60e-2) -	1.0961e+0 (4.34e-2) -	1.0023e+0 (2.95e-2) -	9.2885e-1 (7.73e-2) -	7.0251e-1 (3.68e-2) -	**5.1763e-1 (2.86e-2)**
	8	1.3806e+0 (6.16e-2) -	1.0647e+0 (1.18e-1) -	1.3511e+0 (4.68e-2) -	1.2213e+0 (6.49e-2) -	1.0326e+0 (8.34e-2) -	8.9320e-1 (6.07e-2) -	**7.0378e-1 (4.84e-2)**
	10	1.5885e+0 (7.92e-2) -	1.2327e+0 (1.54e-1) -	1.5629e+0 (6.35e-2) -	1.3502e+0 (5.74e-2) -	1.0654e+0 (1.67e-1) -	1.1753e+0 (1.37e-1) -	**7.9786e-1 (5.24e-2)**
WFG4	3	5.0454e-1 (1.96e-2) -	4.0212e-1 (2.54e-2) -	5.3244e-1 (4.76e-2) -	5.2092e-1 (2.18e-2) -	5.5076e-1 (3.29e-2) -	3.5000e-1 (7.42e-2) ≈	**3.1452e-1 (2.34e-2)**
	4	7.2238e-1 (3.35e-2) -	6.9787e-1 (1.07e-1) -	1.0376e+0 (1.25e-1) -	7.7929e-1 (3.61e-2) -	9.0662e-1 (4.12e-2) -	5.1736e-1 (1.08e-1) ≈	**4.9357e-1 (1.97e-2)**
	6	1.4586e+0 (1.93e-1) -	2.3440e+0 (4.22e-1) -	2.9210e+0 (2.27e-1) -	1.5232e+0 (9.02e-2) -	1.7255e+0 (8.51e-2) -	1.2699e+0 (3.10e-1) ≈	**1.1501e+0 (2.03e-1)**
	8	3.0577e+0 (5.62e-1) -	4.9294e+0 (7.13e-1) -	5.5583e+0 (5.53e-1) -	**2.2800e+0 (1.86e-1) ≈**	2.4239e+0 (7.79e-2) ≈	2.5821e+0 (8.97e-1) ≈	2.5567e+0 (7.64e-1)
	10	4.8541e+0 (7.02e-1) ≈	7.1259e+0 (8.91e-1) -	8.0743e+0 (3.30e-1) -	3.0226e+0 (8.08e-1) +	**2.8549e+0 (8.51e-2) +**	3.5659e+0 (1.46e+0) +	5.1560e+0 (8.06e-1)
WFG5	3	4.1536e-1 (3.73e-2) +	4.9499e-1 (5.67e-2) +	7.0422e-1 (1.55e-2) -	4.3517e-1 (3.65e-2) +	3.5776e-1 (3.31e-2) +	**2.7942e-1 (6.46e-2) +**	5.6211e-1 (6.12e-2)
	4	6.7744e-1 (7.67e-2) +	7.6739e-1 (5.24e-2) ≈	1.0292e+0 (5.50e-2) -	8.0877e-1 (6.04e-2) ≈	6.8285e-1 (4.54e-2) +	**4.5841e-1 (6.39e-2) +**	7.7804e-1 (5.14e-2)
	6	1.4009e+0 (2.67e-1) ≈	1.9977e+0 (2.56e-1) -	2.2387e+0 (1.77e-1) -	1.9196e+0 (9.41e-2) -	2.0425e+0 (2.59e-1) -	1.5733e+0 (1.67e-1) -	**1.3067e+0 (6.16e-2)**
	8	3.0410e+0 (5.32e-1) -	3.7936e+0 (5.14e-1) -	4.2455e+0 (2.60e-1) -	3.6419e+0 (2.49e-1) -	4.2326e+0 (4.31e-1) -	3.2380e+0 (3.12e-1) -	**2.0256e+0 (1.36e-1)**
	10	3.8181e+0 (8.89e-1) -	5.6131e+0 (7.33e-1) -	6.2494e+0 (4.42e-1) -	5.4252e+0 (3.29e-1) -	6.5985e+0 (4.77e-1) -	4.7148e+0 (4.07e-1) -	**2.4663e+0 (2.88e-1)**
WFG6	3	6.9993e-1 (5.37e-2) -	6.6428e-1 (5.39e-2) -	8.5670e-1 (3.25e-2) -	4.6616e-1 (2.72e-2) -	4.7640e-1 (5.49e-2) -	6.4118e-1 (8.27e-2) -	**2.8873e-1 (1.84e-2)**
	4	9.2913e-1 (5.86e-2) -	9.6718e-1 (7.59e-2) -	1.1966e+0 (4.64e-2) -	7.3758e-1 (4.74e-2) -	6.8611e-1 (9.02e-2) -	8.3951e-1 (3.89e-2) -	**4.2705e-1 (1.78e-2)**
	6	1.4193e+0 (9.51e-2) -	1.7441e+0 (2.05e-1) -	2.4449e+0 (1.60e-1) -	1.4635e+0 (2.56e-1) -	1.2210e+0 (2.77e-1) -	1.5514e+0 (9.30e-2) -	**9.0447e-1 (4.38e-2)**
	8	2.3168e+0 (2.85e-1) -	3.6096e+0 (4.15e-1) -	4.5283e+0 (3.54e-1) -	2.5520e+0 (5.10e-1) -	2.2385e+0 (8.46e-1) -	2.6766e+0 (4.86e-1) -	**1.4239e+0 (5.79e-2)**
	10	2.4223e+0 (6.98e-1) -	5.5992e+0 (5.68e-1) -	6.6488e+0 (4.54e-1) -	4.6322e+0 (1.52e+0) -	4.8804e+0 (1.49e+0) -	4.7026e+0 (8.22e-1) -	**1.4981e+0 (5.61e-2)**
WFG7	3	6.8797e-1 (1.96e-2) -	5.0668e-1 (4.00e-2) -	6.3112e-1 (2.11e-2) -	6.0484e-1 (1.92e-2) -	5.9212e-1 (4.20e-2) -	4.8577e-1 (7.01e-2) ≈	**4.5415e-1 (1.18e-2)**
	4	9.2129e-1 (2.85e-2) -	7.6767e-1 (7.31e-2) -	9.6099e-1 (4.04e-2) -	8.9517e-1 (3.38e-2) -	9.3275e-1 (5.23e-2) -	6.8712e-1 (4.60e-2) -	**6.5430e-1 (2.02e-2)**
	6	1.6361e+0 (1.61e-1) -	1.7495e+0 (2.85e-1) -	2.3263e+0 (2.06e-1) -	2.0009e+0 (2.99e-1) -	1.9373e+0 (2.49e-1) -	1.9274e+0 (2.11e-1) -	**1.2408e+0 (1.12e-1)**
	8	3.0647e+0 (4.98e-1) -	3.6967e+0 (4.97e-1) -	4.5875e+0 (3.62e-1) -	3.6753e+0 (7.53e-1) -	3.2629e+0 (5.57e-1) -	3.8363e+0 (4.12e-1) -	**2.4146e+0 (6.22e-1)**
	10	5.0518e+0 (8.22e-1) -	5.6922e+0 (8.71e-1) -	6.6041e+0 (5.61e-1) -	6.4464e+0 (8.19e-1) -	6.5419e+0 (7.70e-1) -	5.9116e+0 (6.55e-1) -	**4.1593e+0 (7.29e-1)**
WFG8	3	6.8711e-1 (5.28e-2) -	6.1778e-1 (4.08e-2) -	7.8153e-1 (3.08e-2) -	7.7916e-1 (2.56e-2) -	7.7823e-1 (3.70e-2) -	6.2150e-1 (4.96e-2) -	**5.6270e-1 (3.34e-2)**
	4	9.5990e-1 (4.93e-2) -	9.5792e-1 (5.48e-2) -	1.2619e+0 (5.72e-2) -	1.1582e+0 (4.00e-2) -	1.1440e+0 (3.34e-2) -	**8.1032e-1 (3.19e-2) +**	8.5249e-1 (4.39e-2)
	6	1.7122e+0 (1.30e-1) -	2.3365e+0 (2.43e-1) -	2.6669e+0 (1.52e-1) -	2.1331e+0 (2.33e-1) -	2.0674e+0 (2.38e-1) -	1.8731e+0 (1.34e-1) -	**1.6151e+0 (8.30e-2)**
	8	3.3971e+0 (2.80e-1) -	4.4000e+0 (2.86e-1) -	4.7831e+0 (2.83e-1) -	3.3738e+0 (3.78e-1) -	3.0181e+0 (6.52e-1) -	3.4864e+0 (4.59e-1) -	**2.6367e+0 (1.96e-1)**
	10	4.4731e+0 (5.17e-1) -	6.4740e+0 (4.33e-1) -	6.8508e+0 (3.56e-1) -	5.7938e+0 (8.97e-1) -	6.1098e+0 (1.32e+0) -	5.1660e+0 (4.32e-1) -	**3.0286e+0 (4.03e-1)**
WFG9	3	8.5736e-1 (6.80e-2) -	7.1356e-1 (8.75e-2) -	8.2537e-1 (4.47e-2) -	7.0815e-1 (7.29e-2) -	6.6614e-1 (6.50e-2) -	5.9190e-1 (1.47e-1) -	**2.2175e-1 (3.57e-2)**
	4	1.2718e+0 (5.53e-2) -	1.0768e+0 (1.12e-1) -	1.2399e+0 (8.72e-2) -	1.1310e+0 (8.89e-2) -	1.1164e+0 (9.24e-2) -	7.6675e-1 (6.87e-2) -	**5.8845e-1 (1.14e-1)**
	6	2.3215e+0 (3.43e-1) -	2.5108e+0 (3.46e-1) -	2.7548e+0 (2.41e-1) -	2.4136e+0 (3.33e-1) -	2.5637e+0 (3.44e-1) -	1.7728e+0 (2.52e-1) -	**1.3036e+0 (2.77e-1)**
	8	4.2938e+0 (5.00e-1) -	4.7855e+0 (5.68e-1) -	4.8888e+0 (2.85e-1) -	4.5197e+0 (5.82e-1) -	4.5802e+0 (5.13e-1) -	3.2770e+0 (3.26e-1) -	**2.3302e+0 (5.33e-1)**
	10	5.7082e+0 (8.74e-1) -	6.8058e+0 (7.59e-1) -	6.9074e+0 (5.04e-1) -	6.7433e+0 (8.34e-1) -	7.2804e+0 (8.32e-1) -	4.9724e+0 (6.83e-1) -	**3.2980e+0 (5.71e-1)**
+/ −/ ≈		2/41/2	6/38/1	0/45/0	2/41/2	3/40/2	5/34/6	

TABLE III

ABLATION RESULTS OF GIMV-SAEA AND ITS VARIANTS ON THE THREE OBJECTIVES DTLZ SUITE IN TERMS OF IGD$^+$ (MEAN AND STD).

Problem	GIMV-LHS	GIMV-KRVEA	GIMV-GA	GIMV-SAEA
DTLZ1	3.1000e+2 (4.69e+1) -	9.5449e-2 (2.85e-3) ≈	9.5526e-2 (2.85e-4) ≈	**9.5442e-2 (3.03e-5)**
DTLZ2	7.5840e-1 (7.58e-2) -	1.0370e-1 (9.12e-3) -	6.8916e-2 (6.07e-3) -	**5.3578e-2 (6.43e-3)**
DTLZ3	9.0291e+2 (1.21e+2) -	2.2338e-1 (1.02e-4) ≈	2.2336e-1 (1.79e-4) ≈	**2.2315e-1 (1.12e-3)**
DTLZ4	6.6914e-1 (1.59e-1) -	1.1349e-1 (9.65e-3) -	7.4522e-2 (1.14e-2) ≈	**6.9979e-2 (7.58e-3)**
DTLZ5	5.8463e-1 (8.34e-2) -	4.4422e-2 (4.67e-3) -	3.0025e-2 (5.93e-3) -	**2.5345e-2 (4.42e-3)**
DTLZ6	9.8632e+0 (7.73e-1) -	9.8857e+0 (9.06e-1) -	1.0410e+1 (6.81e-1) -	**9.1074e+0 (1.09e+0)**
DTLZ7	1.9275e-1 (9.45e-2) ≈	2.1231e-1 (1.40e-1) ≈	1.9358e-1 (1.79e-1) ≈	**1.5950e-1 (7.00e-2)**
+/ −/ ≈	0/6/1	0/4/3	0/3/4	

thus covering the sources of difficulty. As reported in Table III, GIMV-SAEA achieves the best mean IGD$^+$ and outperforms *GIMV-LHS*, *GIMV-KRVEA*, and *GIMV-GA* on 6, 4, and 3 instances, respectively. The results indicate that removing the geometry-guided initialization, the stage-aware training strategy, or the memory-guided variation operator degrades performance to different extents. This trend suggests that the three components play complementary roles in improving initialization quality, surrogate learning, and search effectiveness, and that the advantage of the proposed framework arises from their synergy rather than any single mechanism.

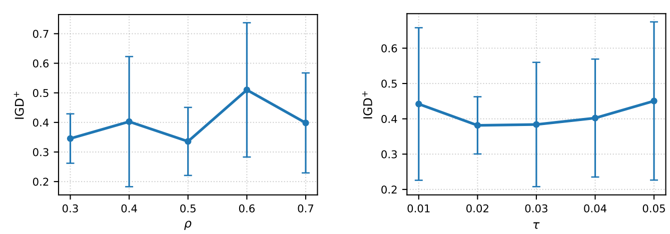

(a) (b)

Fig. 3. Average IGD$^+$ profile plots over different parameter values on the DTLZ7 problem with four objectives based on 20 independent runs. (a) LHS initialization proportion ρ. (b) Diversity threshold τ.

D. Sensitivity Analysis of Parameters

GIMV-SAEA contains two key parameters: the LHS initialization proportion ρ and the diversity threshold τ. We conduct experiments on the DTLZ7 problem with four objectives to analyze the sensitivity of the newly introduced parameters in GIMV-SAEA. The DTLZ7 problem is particularly challenging due to its disconnected Pareto front; hence, it is selected as the test instance in this section.

TABLE IV

IGD$^+$ RESULTS (MEAN $\pm$ STD) OF ORIGINAL AND TSI-ENHANCED BASELINES VS. GIMV-SAEA.

Problem	M	KRVEA	TSI-KRVEA	PIEA	TSI-PIEA	GIMV-SAEA
DTLZ2	3	8.5545e-1 (1.18e-1) −	1.0689e-1 (1.84e-2) −	2.4534e-1 (3.07e-2) −	6.1585e-2 (1.83e-2) ≈	**5.3578e-2 (6.43e-3)**
	10	6.8328e-1 (7.54e-2) −	3.9204e-1 (2.64e-2) −	5.2320e-1 (1.92e-2) −	4.6623e-1 (1.81e-2) −	**2.9682e-1 (3.09e-2)**
MaF13	3	1.3937e+0 (5.58e-1) −	2.5433e-1 (1.33e-2) −	4.9122e-1 (3.70e-2) −	3.9567e-1 (1.58e-2) −	**2.3452e-1 (1.19e-3)**
	10	2.4576e+3 (2.42e+3) −	6.1495e-1 (1.14e-3) −	1.3180e+0 (4.63e-1) −	**5.5855e-1 (1.07e-2)** +	6.1439e-1 (1.57e-3)
WFG9	3	8.5736e-1 (6.80e-2) −	2.5237e-1 (5.13e-2) −	5.9190e-1 (1.47e-1) −	**1.7281e-1 (2.73e-2)** +	2.2175e-1 (3.57e-2)
	10	5.7082e+0 (8.74e-1) −	5.2134e+0 (5.83e-1) −	4.9724e+0 (6.83e-1) −	4.8116e+0 (8.85e-1) −	**3.2980e+0 (5.71e-1)**
+/ −/ ≈		0/6/0	0/6/0	0/6/0	2/3/1	

As illustrated in Fig. 3(a), the smallest mean IGD$^+$ is achieved at $\rho = 0.5$, whereas both smaller and larger values lead to inferior performance and larger variability, indicating that an intermediate proportion provides a better balance between global exploration via LHS and local sampling within early-stage elite regions. Fig. 3(b) shows that $\tau = 0.02$ yields the best or near-best mean performance with relatively stable dispersion, supporting timely switching between exploration- and exploitation-oriented modes.

Other introduced parameters were also tested extensively and showed little influence on the results, indicating that GIMV-SAEA is not overly sensitive to their default settings.

E. Effects of Geometry-Guided Initialization

Since strong initialization may significantly affect the performance of surrogate-assisted algorithms under strict evaluation budgets, we further investigate whether the superiority of GIMV-SAEA stems solely from the proposed geometry-guided three-stage initialization (TSI). To this end, we equip two representative baselines, K-RVEA and PIEA, with the same TSI procedure, while keeping their other components unchanged, and compare them with the original baselines and GIMV-SAEA on several representative test scenarios. Table IV reports the IGD$^+$ results on six representative cases (DTLZ2, WFG9, and MaF13 with $M = 3$ and 10).

The results show that equipping strong baselines with TSI substantially improves their performance in most cases, confirming that initialization plays an important role under limited budgets. Nevertheless, GIMV-SAEA still achieves the best or highly competitive results in the majority of cases, indicating that the performance gains cannot be attributed solely to the initialization and that the proposed stage-aware training strategy and memory-guided variation operator provide additional benefits beyond the initial sampling phase.

F. Robustness Analysis on Offset Problems

When the true PS deviates from the geometric priors, geometry-based initialization may become less effective. To examine the adaptability of GIMV-SAEA to such cases, we construct an *Offset DTLZ* (ODTLZ) testbed based on DTLZ, which contains 21 instances. In ODTLZ, three groups of decision-variable offset values are generated within $[0.1, 0.9]$ using three fixed random seeds, where each group consists of seven offset values corresponding to DTLZ1–7. For DTLZ1–5, the offset is introduced by replacing the original center value (0.5) in the g function with the corresponding offset, thereby translating the latter part of the decision variables. For DTLZ6–7, an absolute-value safeguard is additionally applied after the offset. As a result, the true PS is deliberately displaced away from the boundary- and center-related geometric priors. All 21 ODTLZ instances are evaluated with ten objectives.

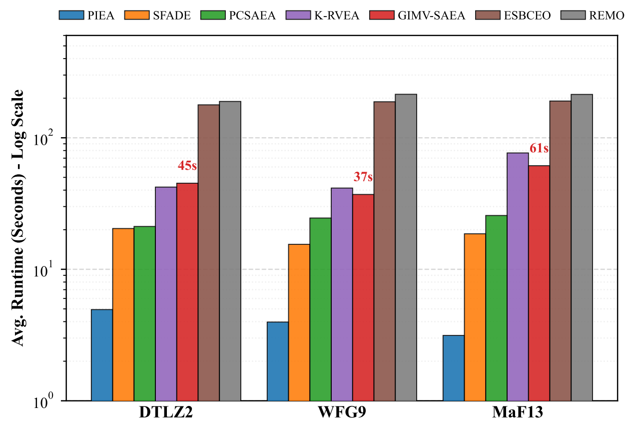

Fig. 4. Average runtime (seconds, logarithmic scale) of different algorithms on DTLZ2, WFG9, and MaF13 with $M = 10$.

According to the IGD$^+$ comparison, GIMV-SAEA achieves 12 wins, 8 ties, and 1 loss against GIMV-LHS. These results further suggest that the performance gain of GIMV-SAEA does not rely solely on favorable geometric priors, but also benefits from the Stage 2 space-filling safeguards and Stage 3 local sampling around early elite regions.

G. Runtime Analysis

To quantify the computational overhead of GIMV-SAEA, we report the average runtime of all algorithms on three representative problems, namely DTLZ2, WFG9, and MaF13 with $M = 10$, under the same evaluation budget.

Fig. 4 summarizes the runtime comparison results. As expected, PIEA runs substantially faster, mainly because its lightweight SVM-based surrogate modeling incurs much lower training overhead than Kriging in the same implementation. By contrast, REMO is consistently slower, likely due to the additional overhead introduced by its relation-learning surrogate and selection procedure. In comparison, GIMV-SAEA exhibits a runtime level comparable to other Kriging-based

TABLE V

HV RESULTS (MEAN AND STANDARD DEVIATION) OBTAINED BY SIX ALGORITHMS ON THE ROCKET INJECTOR DESIGN PROBLEM (RE3–4–7).

KRVEA	REMO	PCSAEA	SFADE	PIEA	**GIMV-SAEA**
5.9655e-1 (1.76e-3) -	6.1219e-1 (2.89e-2) -	5.5085e-1 (2.07e-2) -	5.9702e-1 (6.91e-3) -	6.3702e-1 (2.29e-2) ≈	**6.3841e-1 (2.77e-2)**

methods (e.g., K-RVEA), while achieving better optimization performance, indicating that the proposed stage-aware training mechanism can enhance solution quality without a noticeable increase in runtime.

H. Real-World Engineering Application

Table V presents the HV results on the Rocket Injector Design problem (RE3–4–7) [24], a real-world EMOP with 4 decision variables and 3 objectives. Under a strict budget of $FE_{\max} = 300$, GIMV-SAEA obtains the highest mean HV and is statistically comparable to PIEA, while significantly outperforming classical baselines such as K-RVEA and REMO. These results demonstrate that GIMV-SAEA can effectively obtain high-quality trade-off solutions in complex real-world engineering applications under a strict evaluation budget.

V. CONCLUSION

To address cold-start and inefficient evolution in EMOPs, this paper proposed GIMV-SAEA. By combining boundary probing, a central anchor, LHS-based space-filling sampling, and elite-guided local sampling, the proposed method improves initialization quality under limited evaluation budgets. The evolution-stage-aware training set construction mechanism and the memory-guided adaptive variation operator further enhance the balance between surrogate modeling efficiency and search effectiveness. Experimental results on standard benchmark suites, offset test instances, and a real-world engineering problem demonstrate that GIMV-SAEA achieves competitive convergence performance and robustness. Moreover, the runtime analysis indicates that these performance gains are obtained without a noticeable increase in runtime under strict evaluation budgets. Future work will extend GIMV-SAEA to expensive constrained multi-objective optimization and broader engineering applications.

REFERENCES

[1] H. Wang, Y. Jin, and J. O. Jansen, "Data-driven surrogate-assisted multiobjective evolutionary optimization of a trauma system," *IEEE Trans. Evol. Comput.*, vol. 20, no. 6, pp. 939–952, 2016.

[2] Z. Lu, I. Whalen, V. Boddeti, Y. Dhebar, K. Deb, E. Goodman, and W. Banzhaf, "NSGA-Net: Neural architecture search using multi-objective genetic algorithm," in *Proc. Genet. Evol. Comput. Conf.*, 2019, pp. 419–427.

[3] M. D. McKay, R. J. Beckman, and W. J. Conover, "A comparison of three methods for selecting values of input variables in the analysis of output from a computer code," *Technometrics*, vol. 21, no. 2, pp. 239–245, 1979.

[4] D. G. Krige, "A statistical approach to some basic mine valuation problems on the Witwatersrand," *J. South. Afr. Inst. Min. Metall.*, vol. 52, no. 6, pp. 119–139, 1951.

[5] Y. Jin, "Surrogate-assisted evolutionary computation: Recent advances and future challenges," *Swarm Evol. Comput.*, vol. 1, no. 2, pp. 61–70, 2011.

[6] L. Pan, C. He, Y. Tian, H. Wang, X. Zhang, and Y. Jin, "A classification-based surrogate-assisted evolutionary algorithm for expensive many-objective optimization," *IEEE Trans. Evol. Comput.*, vol. 23, no. 1, pp. 74–88, 2019.

[7] T. Chugh, Y. Jin, K. Miettinen, J. Hakanen, and K. Sindhya, "A surrogate-assisted reference vector guided evolutionary algorithm for computationally expensive many-objective optimization," *IEEE Trans. Evol. Comput.*, vol. 22, no. 1, pp. 129–142, 2018.

[8] Y. Li, W. Li, S. Li, and Y. Zhao, "A performance indicator-based evolutionary algorithm for expensive high-dimensional multi-/many-objective optimization," *Inf. Sci.*, vol. 678, p. 121045, 2024.

[9] J. Knowles, "ParEGO: A hybrid algorithm with on-line landscape approximation for expensive multiobjective optimization problems," *IEEE Trans. Evol. Comput.*, vol. 10, no. 1, pp. 50–66, 2006.

[10] Q. Zhang, A. Zhou, and Y. Jin, "RM-MEDA: A regularity model-based multiobjective estimation of distribution algorithm," *IEEE Trans. Evol. Comput.*, vol. 12, no. 1, pp. 41–63, 2008.

[11] R. Cheng, Y. Jin, M. Olhofer, and B. Sendhoff, "A reference vector guided evolutionary algorithm for many-objective optimization," *IEEE Trans. Evol. Comput.*, vol. 20, no. 5, pp. 773–791, 2016.

[12] K. Deb, A. Pratap, S. Agarwal, and T. Meyarivan, "A fast and elitist multiobjective genetic algorithm: NSGA-II," *IEEE Trans. Evol. Comput.*, vol. 6, no. 2, pp. 182–197, 2002.

[13] Y. Horaguchi, K. Nishihara, and M. Nakata, "Evolutionary multiobjective optimization assisted by scalarization function approximation for high-dimensional expensive problems," *Swarm Evol. Comput.*, vol. 86, p. 101516, 2024.

[14] H. Bian, J. Tian, J. Yu, and Y. Han, "Bayesian co-evolutionary optimization based entropy search for high-dimensional many-objective optimization," *Knowl.-Based Syst.*, vol. 274, p. 110630, 2023.

[15] Y. Tian, J. Hu, C. He, H. Ma, L. Zhang, and X. Zhang, "A pairwise comparison based surrogate-assisted evolutionary algorithm for expensive multi-objective optimization," *Swarm Evol. Comput.*, vol. 80, p. 101323, 2023.

[16] H. Hao, A. Zhou, H. Qian, and H. Zhang, "Expensive multiobjective optimization by relation learning and prediction," *IEEE Trans. Evol. Comput.*, vol. 26, no. 5, pp. 1157–1170, 2022.

[17] K. Deb, L. Thiele, M. Laumanns, and E. Zitzler, "Scalable test problems for evolutionary multiobjective optimization," in *Evolutionary Multiobjective Optimization: Theoretical Advances and Applications*, 2005, pp. 105–145.

[18] S. Huband, P. Hingston, L. Barone, and L. While, "A review of multiobjective test problems and a scalable test problem toolkit," *IEEE Trans. Evol. Comput.*, vol. 10, no. 5, pp. 477–506, 2006.

[19] R. Cheng, Y. Jin, M. Olhofer, and B. Sendhoff, "Test problems for large-scale multiobjective and many-objective optimization," *IEEE Trans. Cybern.*, vol. 47, no. 12, pp. 4108–4121, 2017.

[20] Y. Tian, R. Cheng, X. Zhang, and Y. Jin, "PlatEMO: A MATLAB platform for evolutionary multi-objective optimization," *IEEE Comput. Intell. Mag.*, vol. 12, no. 4, pp. 73–87, 2017.

[21] H. Ishibuchi, H. Masuda, Y. Tanigaki, and Y. Nojima, "Modified distance calculation in generational distance and inverted generational distance," in *Evolutionary Multi-Criterion Optimization*, 2015, pp. 110–125.

[22] E. Zitzler, L. Thiele, M. Laumanns, C. M. Fonseca, and V. G. da Fonseca, "Performance assessment of multiobjective optimizers: An analysis and review," *IEEE Trans. Evol. Comput.*, vol. 7, no. 2, pp. 117–132, 2003.

[23] J. Derrac, S. Garcia, D. Molina, and F. Herrera, "A practical tutorial on the use of nonparametric statistical tests as a methodology for comparing evolutionary and swarm intelligence algorithms," *Swarm Evol. Comput.*, vol. 1, no. 1, pp. 3–18, 2011.

[24] R. Tanabe and H. Ishibuchi, "An easy-to-use real-world multi-objective optimization problem suite," *Appl. Soft Comput.*, vol. 89, p. 106078, 2020.